

## AERODYNAMIC DESIGN OF WINGS WITH REALISTIC PLAN FORM THROUGH OPTIMIZATION TECHNIQUES

**Pedro Paglione** – e-mail: [paglione@era.ita.cta.br](mailto:paglione@era.ita.cta.br)

**Roberto M. Girardi** - e-mail: [girardi@aer.ita.cta.br](mailto:girardi@aer.ita.cta.br)

Instituto Tecnológico de Aeronáutica (ITA)

Praça Mal. Eduardo Gomes, 50 - 12.228-900 São José dos Campos, SP.

**Abstract** *Modern wing plan forms are characterized by a kink in some place along the wing span, used to solve practical problems associated with the positioning of landing gear and aeronautical systems (such as hydraulic, fuel and anti-ice systems) inside the wing. A method for designing such wings, based on optimization techniques is presented in the present paper. An optimization code and an aerodynamic code, based on the well known vortex lattice method, are combined. The objective of the optimization procedure is the minimization of the induced drag and some constraints are imposed to be satisfied during this procedure, in order to avoid non practical solutions. The Bandeirante aircraft wing was used as the initial condition of the optimization procedure and two wing designs, subjected to two different sets of constraints, were obtained. A kink station was observed in both solutions and induced drag values were lower than the value calculated for the Bandeirante wing. Moreover, the designed wings have lower plan form area, which is advantageous because the profile drag is proportional to such area.*

**Key-words:** Wing design, Optimization technique, Induced drag

### 1. INTRODUCTION

It is well known in aeronautics engineering that an elliptic circulation distribution along the wing span is correlated to the minimum value for the induced drag coefficient. Such distribution is obtained for an elliptic plan form wing. Although this plan form had been used in practice, it is difficult to manufacture, integration of control surfaces to the wing, like slats, flaps and aileron, are more complicated and good design solutions to accommodate the landing gear, fuel tanks and anti-ice systems inside the wing are not possible. The above problems are more easily solved by using wings with straight leading and trailing edges and allowing a kink at some station along the wing span. In such cases, the wing is constituted by an internal part, which is limited by the root and kink stations and an external one, beginning at the kink station and going to the wing tip. Each part may have different values for the sweep back angle, for the aerodynamic and geometric twist, for the taper ratio, as well as, each station may have a different kind of aerodynamic profile.

The above parameters are considered in the wing design performed in the present work, whose objective is to present a design methodology to obtain wings with minimum induced

drag. In order to accomplish this objective, an aerodynamic code for calculating a wing, characterized with a kink station, is developed and used as a subroutine of an optimization code, which performs the optimization of some objective function (in the present case, the minimization of the induced drag) restricted by a set of constraints, used to avoid undesirable characteristics.

Incompressible and potential flow is considered in the present work. In this case, the panel method (see Hess & Smith, 1966) can be used to model the flow over a wing, considering all the design parameters mentioned above. Every profile characteristics are considered and the pressure distribution can be calculated with good accuracy. With this method, the so called “profile drag” can be calculated by using boundary layer theory. On the other hand, the wing surface has to be well discretized and the computational effort is incremented.

During the optimization procedure, the analysis code is called hundreds of times in order to find the extreme value required, such as, for example, the minimum induced drag. In this case, the aerodynamic code must be as fast as possible, at least for the first steps of a conceptual design, where several configurations have to be analyzed. Due to this constraint, the “Vortex Lattice” method becomes a good choice, because the lifting surface theory (see Schlichting & Truckenbrodt, 1979) produces very good results for the aerodynamic parameters. With this method, the profile drag can not be calculated with accuracy, because the pressure distribution over the wing surface is poor.

The optimization strategy used in this work was developed by Jacob (1982) and it is accomplished in two steps: In the first one, a code called “Extreme” is used to find a local extreme point, that is, given an initial configuration the nearest minimum is found for the objective function, which, in the present case, is the induced drag. In the second step, the initial configuration is changed and the “Extreme” code is called again. This operation is performed by a code called “Globex”, which is responsible for finding the global extreme value of the objective function.

Finally, the wing of the Bandeirante aircraft is used as an example for the design procedure mentioned above. Considering different sets of constraints, two optimal wings were obtained with distinct plan forms.

## **2. AERODYNAMIC ANALYSIS OF A WING**

As mentioned above, the “Vortex Lattice” method is used in the present work to model the incompressible and potential flow over a finite wing. This method is restricted by the small perturbation theory hypotheses. The profile thickness is not considered, the angle of attack has to be small and the singularities are distributed on the chord plane, although the profile camber line is considered to calculate the wing surface normal direction, which is used to enforce the boundary conditions.

The vortex lattice method is based on the horse shoe vortex singularity (see Schlichting & Truckenbrodt, 1979), placed on each element of a wing discretization, as shown in the figure 1. The wing span is divided in  $N_s$  strips, which are sub-divided in  $N_c$  elements, resulting a discretization with  $N_s \times N_c$  elements. Simpler methods for wing analysis use just in discretization along the wing span. Although the chordwise discretization increases the computational run time, it is important because the profile camber line can be considered in the flow calculations, as well as some parameters can be obtained from the numerical solution, such as the pitch moment coefficient and the center of pressure position.

The unknowns of the numerical problem are the circulation intensity of each vortex shoe singularity. These unknowns are determined by solving a system of  $N_s$  times  $N_c$  equations,

which are obtained by imposing the boundary condition at each element of the discretization. To enforce this boundary condition, the velocity at the control point of a certain element, induced by all vortex sheet singularities, distributed on the wing surface, are considered together with the undisturbed flow velocity, in order to force the flow to be tangent to the profile camber line, that is, the normal velocity at each control point has to be equal to zero. Once the singularity intensities are obtained, the circulation at each strip along the wing span can be calculated. Using this circulation distribution, the lift along the wing span can be obtained by utilizing the Kutta & Joukowski theorem (see Karamcheti, 1980). Additionally, the values of all other parameters can be determined along the wing span, such as the induced angle, induced drag, pitch moment and the center of pressure location. Finally, the above parameters can be integrated along the wing span to obtain the aerodynamic coefficients of the wing under consideration.

In the numerical code developed in this work, the wing plan form has a realistic shape, where the leading and trailing edge are straight lines, but a kink of these lines can occur at a certain position along the wing span, between the root and the tip sections, as shown in the figures 3 and 6. The geometrical parameters describing the wing plan form are the following: root chord ( $C_r$ ), kink chord ( $C_k$ ), tip chord ( $C_t$ ), wing span ( $B$ ), span related to the kink section ( $B_i$ ), sweep angle of the internal and external parts of the wing ( $\phi_i$ ) and ( $\phi_e$ ), respectively. The same profile is considered along the whole wing span and a four-digit NACA family is used in the present paper. The code has an option to use a generic profile, whose shape is defined by a set of coordinates. The angles of attack for the root ( $\alpha_r$ ), for the kink ( $\alpha_k$ ) and for the tip stations ( $\alpha_t$ ) are entry parameters, which are used to define the internal and external twist angle variation, considered linear for each wing part.

### 3. OPTIMIZATION METHOD

The optimization technique can be mathematically stated as the following optimization problem:

$$J = \max[F(x)] \tag{1}$$

$$\text{subject to } g_i(x) \leq 0, \quad i = 1, 2, \dots, q$$

where  $x$  is a vector containing the design variables and  $J$ , figure of merit of this problem, is the induced drag of a wing. The term  $g_i(x)$  defines all the  $q$ -constraints pertinent to the problem as described below.

For obtaining the optimal wing according to a specific aerodynamic figure of merit (minimum induced drag) serving as the objective function, the numerical optimization procedure Globex, implemented by Jacob (1982), is used in this work. It employs a robust local minimization algorithm of a real valued function of several variables that converge quickly to the nearest relative extreme point insensitive to curved valleys and sharp ridges in the variables-criterion space and can handle any type of constraint with no need of gradients evaluation, since each time a constraint violation is detected, the optimization algorithm is signalled to provide a new set of variables until a set is obtained that violates no boundary.

For aerodynamic optimization this is an advantageous strategy, besides its simplicity, since the gradients evaluation could have a prohibitive computational cost due to iterative procedures or even be impossible in some particular cases. The global extreme of the function is reached, with great likelihood, through the use of a three step procedure based on a normally distributed random number. In the first step, the initial values of the variables are

estimated. The vectorial mean value of these normally distributed points as well the mean quadratic deviation is derived from the user initial points given. In each one of these points, a local extremization procedure is started. In the second step, around the variables that resulted in the best function value, once more normally distributed random numbers are generated and in each one of the these points a new local optimization is calculated. Once a better function value is found, this point is used as the new mean value for another random search and the mean quadratic deviations are multiplied by 0.9 (localization of the global extreme). The best of all in these both step found point is stored and used as the initial value for a third optimization step. Although the global extreme can not be determined with absolute security, the probability that it is found increases with the number of random estimated values.

#### 4. ANALYSIS OF RESULTS

The study conducted in the present work is based on the wing used on the first airplane designed by EMBRAER, called the Bandeirante. The initial configuration at the beginning of the optimization procedure is always the wing mentioned above. Additionally, the lift produced by the wing ( $L$ ), as well as, the span value ( $B$ ) for all wings presented in this paper have the same value and they are equal to those of the Bandeirante wing. Therefore, this wing has to be considered as the first step of the present research and its characteristics are presented in table 1 and figure 1. It is important to mention that such a wing has no kink in its trapezoidal plan form, no geometric twist and the no aerodynamic twist, because the root and tip section airfoils have the same camber line characteristics.

Bandeirante wing

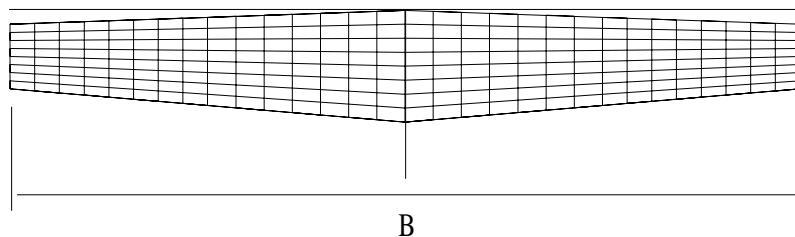


Figure 1 Bandeirante wing plan form

The circulation distribution along the wing span for the Bandeirante wing and for an elliptical wing with the same lift coefficient ( $C_l$ ) and the same aspect ratio ( $A$ ) as the Bandeirante one are presented in figure 2 (a). It is important to mention that the undisturbed flow velocity ( $V_\infty$ ) and span ( $B$ ) are used to obtain the non-dimensional circulation shown in the figure 2 (a), where a small difference can be observed between the two wings. Due to this difference the Bandeirante wing has a greater induced drag coefficient ( $C_{di}$ ) than the elliptic wing with the same  $C_l$  and  $A$ . The wing  $C_{di}$  is obtained through an integration along the span of the local induced drag coefficient shown in the figure 2 (b). At the internal part of the wing span, the induced drag associated to the Bandeirante wing is lower than that of the elliptic wing. The opposite can be observed for the region near the wing tip. This result is correlated to the circulation distribution shown in the figure 2 (a).

In the present work, the optimization objective is to minimize the induced drag ( $D_i$ ) of a wing subjected to certain constraints:

- The root chord has to be greater than that of the tip ( $C_t$ ), as well as, the kink chord ( $C_k$ );

- The sweep back angles (internal,  $\varphi_i$  , and external,  $\varphi_e$  ) have to be lower than 50 degrees;
- The angles of attack for the wing stations at the root ( $\alpha_r$  ), at the kink ( $\alpha_r$  ) and at the tip ( $\alpha_r$  ) have to be between  $-4$  and  $+4$  degrees;
- The lift produced by the wing has to be greater than 49.000 N;
- The span (B) has to be lower than 16.5 m;
- The span referred to the kink station (Bi) has to be between 2.2 and 14.3 m;
- The maximum value for the local lift coefficient distribution has a value between 0.3 and 0.5 of the semi-span (Roskam, 1985). This constraint is important because it fixes the station where the stall begins, avoiding problems with the control surface, positioned at the wing tip region.

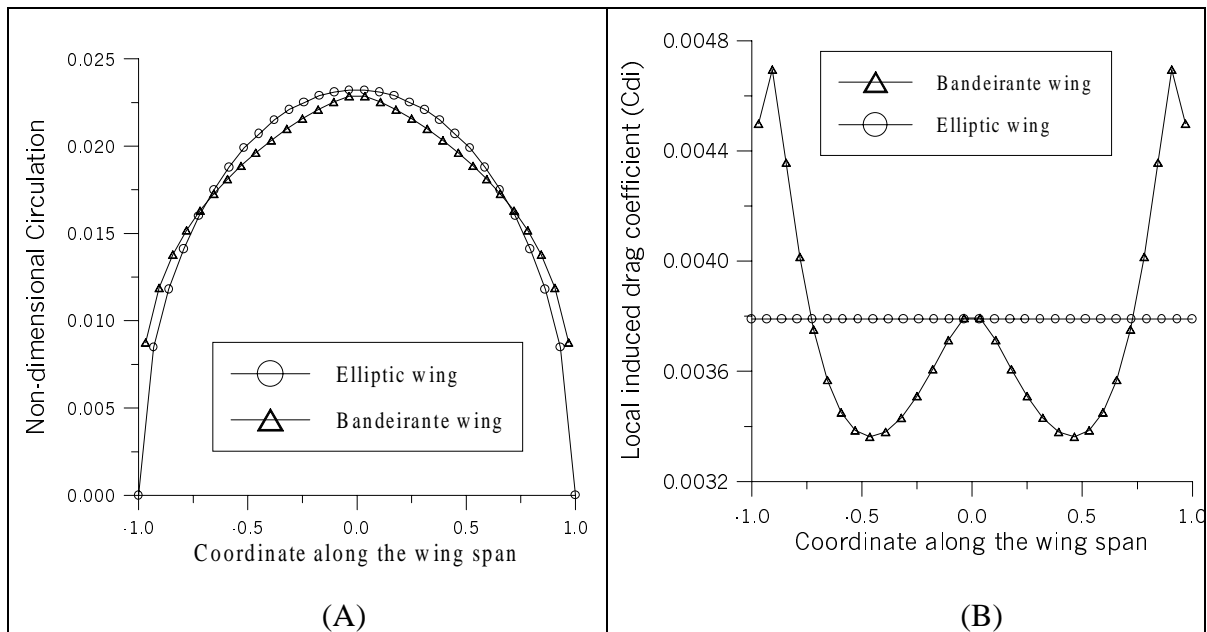


Figure 2: (A) Circulation and (B) local induced drag distributions along the span of the Bandeirante wing.

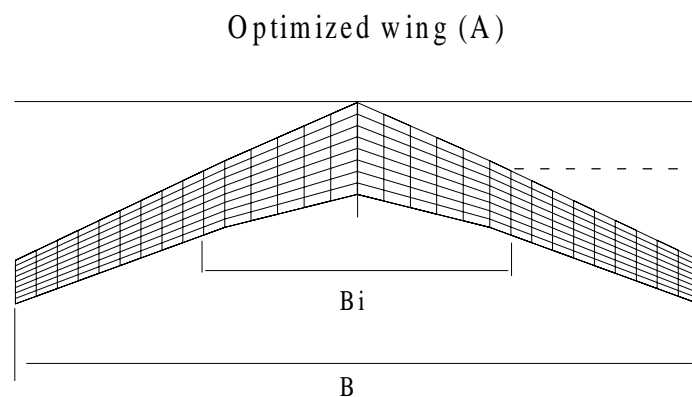


Figure 3: Plan form of the optimized wing – case (A)

The plan form of the first result obtained by the optimization procedure (case – A) is shown in the figure 3 and the numerical results for several parameters are presented in tables

1 and 2. The wing is characterized by a soft kink located at 38.8% of the semi-span and by high values for the sweep back angles. This is an unexpected result because the sweep back angle increment is normally associated to a decrease of the  $dC_l/d\alpha$  and to maximum value of local lift coefficient near the wing tip. Additionally, for wings without twist and for a fixed value of  $C_l$ , the induced drag coefficient has a lower value for a rectangular wing than for a sweep back one.

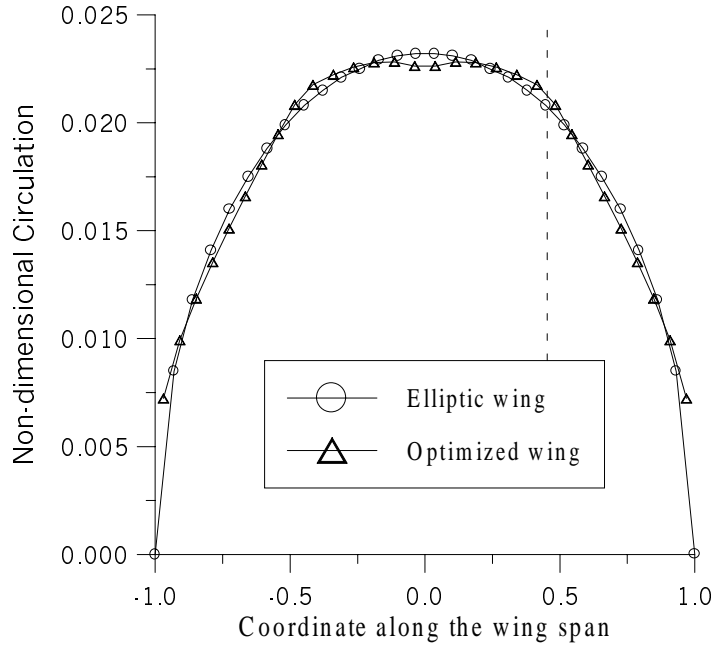


Figure 4: Circulation distribution along the span for the optimized wing – case (A)

The circulation distributions along the span for the optimized wing and for an elliptic wing are almost coincident, as can be observed in the figure 4. The several controls (i.e., the parameters mentioned in the preceding section) are modified by the optimization procedure in order to approach the circulation distribution to the ideal, which is the elliptic distribution. The dashed line in figure 4 indicates the position of the kink station and no discontinuities are observed, as could be expected.

A comparison between the optimized wing (A) and that of the Bandeirante can be performed with the results presented in the tables 1 and 2. Every chord of the optimized wing was decreased relative to the Bandeirante. The span reaches its maximum value allowed by the constraint mentioned before and this result was expected, because an increment of the aspect ratio causes a decrement of the induced drag coefficient. The optimized wing area is lower than the Bandeirante and this fact is a consequence of the chords decrement. As the span value is the same for both wings, the area decrement is the cause of the greater value obtained for the aspect ratio of the optimized wing.

An important parameter for fitting the circulation distribution to the elliptic one is the twist along the wing span. Along the internal part of the wing span, that is, from the root station to the kink one, a small increment for the angles of attack can be observed meanwhile the opposite result is observed to the external part, with a pronounced variation of the angle values. Considering that the wing plan form has almost a trapezoidal shape, the kink station is useful to allow different variations for the twist of the internal and external parts of the wing span.

Table 1: Geometric characteristics of the wings plan form

Wing	Cr (m)	Ck (m)	Ct (m)	Bi/B	$\phi_i$ (degree)	$\phi_e$ (degree)	S (m <sup>2</sup> )	A
Bandeirante	2.33	1.84	1.35	-	2.0	2.0	30.0	9.0
(A)	2.21	1.60	1.05	38.8	23.7	25.4	25.6	10.6
(B)	1.93	1.50	0.70	45.3	15.4	5.2	22.8	12.0

Table 2: Geometric twist and aerodynamic characteristics of the wings

Wing	$\alpha_r$ (degree)	$\alpha_k$ (degree)	$\alpha_t$ (degree)	Cl	Cm	Cdi	Di (N)
Bandeirante	2.3	2.3	2.3	0.33	-0.062	0.0037	556
(A)	3.1	3.5	1.1	0.39	-0.045	0.0043	530
(B)	3.2	3.4	2.6	0.44	-0.053	0.0049	549

Relative to the Bandeirante wing, the lift coefficient for the optimized wing (A) has a greater value and this is a direct consequence of the decrement of the optimized wing area, because the lift value can not be lower than 49.000 N (see constraints described above). The increment of Cl is also an unexpected result, because the induced drag coefficient is a function of  $Cl^2$ . An increment of the wing area would result in a decrement of Cl and therefore a decrement of Cdi. On the other hand, as the span value is limited, an increment of the wing area causes a decrement of the aspect ratio (A), and then an increase of Cdi. Additionally, it must be remembered that the optimization objective is to minimize the induced drag (Di), which is dependent on both the induced drag coefficient (Cdi) and on the wing area (S). Thus, the above reasoning seems to explain why the optimization procedure make the choice of decreasing the wing area to reach its objective.

The pitch moment coefficient has just a small variation, which is a consequence of changes on both the maximum camber ratio and the position this maximum take along the profile chord. It is important to mention that no constraints were necessary to keep this parameter within a range of reasonable values.

The induced drag coefficient (Cdi) and Di are connected by the wing area. Thus, although Cdi for the optimized wing is greater than for the Bandeirante one, the induced drag (Di) for the optimized wing has a lower value, with a decrement of approximately 5%.

The total wing drag for the optimized wing would have a greater reduction, because the so called profile drag has to be considered and such a parameter is proportional to the wing area, which is approximately 17% lower than the Bandeirante, as can be seen in table 1.

The local lift coefficient distribution along the span is very important to verify the station where the stall will start when the wing angle of attack is incremented. This station can not be at the wing tip region to avoid problems with the control surface present at that region of the wing span. The results obtained for the optimized wing (A) and for the Bandeirante are presented in figure 5 (a), where the local Cl is divided by the wing total lift coefficient (CLt) in order to allow the comparison of different wings. The optimized wing is characterized by lower values of Cl over the internal part. This result shows that the stall would run toward the wing tip, before it goes toward the root and this is an undesirable behavior. The dashed line also indicates the kink station position, which is near the position for the maximum local value of Cl, but not coincident. Again, no discontinuity is observed as expected due to the changes in the twist angle.

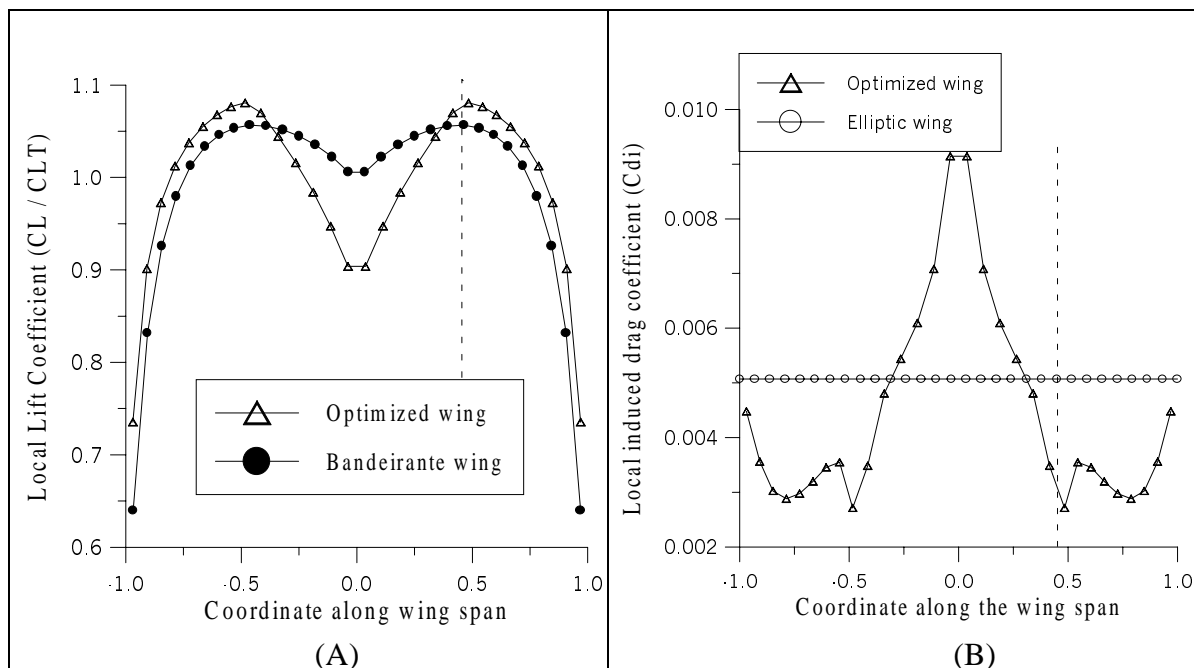


Figure 5: (A) Local lift coefficient and (B) induced drag coefficient distributions along the span for the optimized wing – case (A)

The local induced drag distribution for the optimized wing (A) is presented in the figure 5 (b) together with the results for an elliptic wing, which has the same values for the CL and A of the optimized one. On the contrary to the Bandeirante results (see Fig. 2 b), the internal part of the wing span contributes more to the total induced drag than the external part. Near the kink station (dashed line position) the Cdi distribution is characterized by an oscillation which is certainly connected to the small changes observed in figure 4.

As analyzed before, the decrement of the wing area, for a fixed value of the lift, results in the increment of the total lift coefficient and, as a consequence, the incremented of the induced drag coefficient (Cdi). On the other hand, the induced drag (Di) can diminish and, due to the area variation, the profile drag certainly has a decrement. Such variation for the profile drag is very interesting and this is the motivation for researching another wing, with an area lower than the value obtained for the optimized wing (A), discussed above.

Optimized wing (B)

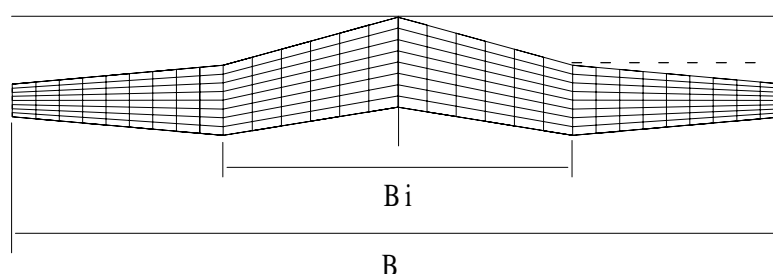


Figure 6: Plan form of the optimized wing – case (B)

For the wing above, all the constraints considered before have to be satisfied and, additionally, a superior limit for the wing area is fixed with the value of 22.8 m<sup>2</sup>. The optimization procedure with this additional constraint obtained the wing plan form shown in



figure 6, where a pronounced plan form kink can be observed. For the internal part of the span, the sweep back angle has a great value, approximately 15 degrees, but for the external part, a small angle was obtained, as can be seen in the table 1.

The circulation distribution along the span for the optimized wing (B) and for an elliptic wing, which has the same values of lift coefficient and aspect ratio of the optimized wing, are shown in the figure 7 (a). As in the preceding case, the optimization procedure has found a set of parameters which produces a circulation distribution almost coincident with the elliptic one. The dashed line, observed in the figure 7 (a), indicates the kink station position and, again, no discontinuity is detected, although the plan form has a pronounced discontinuity.

It is very difficult to explain why the optimization procedure has chosen the specific plan form shown in the figure 6 but, the dashed line observed in the figure 7 (a) seems to separate the circulation distribution into two parts: the internal one with a small variation and the external part, where a great variation can be verified. As expected, the aspect ratio (A) is greater and the chords ( $C_r$ ,  $C_k$  and  $C_t$ ) are lower than the same parameters of the optimized wing (A), as can be seen in the table 1. The tip chord ( $C_t$ ) had a greater change than the other chords and, as a consequence, the taper ratio of the external part was incremented, relative to the optimized wing (A).

A suitable characteristic of the optimized wing (B) is the twist angles, mainly the one for the external part of the span, as can be seen in the table 2. Relative to the Bandeirante, the present wing case has an area approximately 30% lower and induced drag ( $D_i$ ) also lower (about 1.3%). Such a result is very interesting because the profile drag must be reduced approximately the same amount as the area. It must be remembered that the profile drag is a function of the Reynolds number, which is certainly lower than the Bandeirante, due to the reduction of the profile chords.

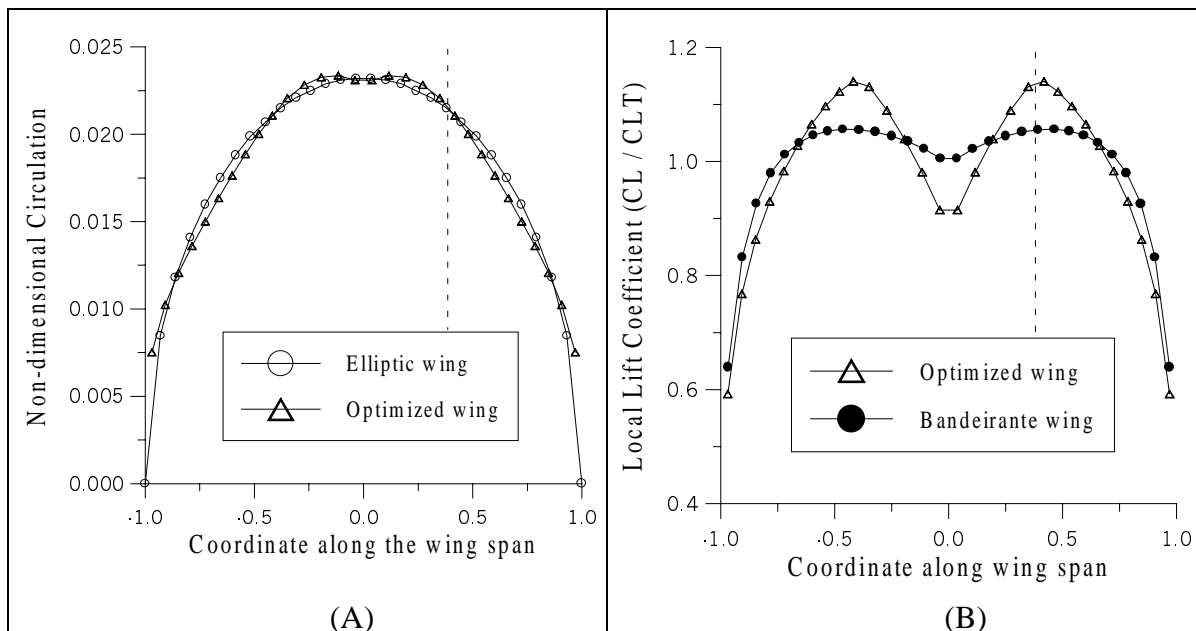


Figure 7: (A) Circulation and (B) local lift coefficient distributions along the span for the optimized wing – case (B)

The local lift coefficient for the optimized wing (B), shown in the figure 7 (b), is very similar to the one found for the case (A). The pronounced maximum value for  $CL$  is a bad characteristic, because the wing will start to stall at low values of the total lift coefficient and,

therefore the stall velocity will be high. Due to this fact, high lift devices have to be more complex and expensive, in order to make the landing and take off operations safer.

## 5. FINAL REMARKS

The present work is the first step of a research program whose final objective is the performance of multi-disciplinary optimization (MDO) in the area of aircraft design. In the present paper, just aerodynamic optimization was considered and the wing optimization of the Bandeirante aircraft was performed.

Considering that the aerodynamic and optimization codes are developed and validated, the optimization procedure consists in finding: (i) an objective function, which in the present case is the minimization of the induced drag and (ii) the constraints required to avoid non practical solutions. The question associated with the constraints is not as simple as expected at the beginning of the work. In fact, some constraints were implemented while the work was developing, in order to correct undesirable solutions that the optimization procedure obtains and, this interactive procedure is very useful for a better understanding of the problem under treatment.

In the first solution reported in this paper (case-A) the area was lower than the initial one, which was the Bandeirante wing area. This result was obtained without a constraint of this parameter and it is a consequence of the chosen objective function, that is, minimization of the induced drag ( $D_i$ ). If the induced drag coefficient ( $C_{di}$ ) was chosen as the objective function, then the wing area would be as large as possible, in order to obtain a decrement of the lift coefficient, which is strongly connected to  $C_{di}$ , as mentioned before.

The second solution, the optimized wing (B), was obtained with a constraint on the wing area, in order to diminish the profile drag. A completely different plan form wing was obtained, the lift and induced drag coefficients were incremented but the induced drag was still lower than the Bandeirante wing.

In both solutions described above, the local lift coefficient distribution has a sharp maximum and this is an undesirable characteristic, because the beginning of stall will occur for low values of the total lift coefficient. Such a shortcoming can be corrected by implementing new constraints, which certainly will produce a different wing.

In future works, the aerodynamic code will be improved in order to consider different profile shapes along the wing span and the profile drag, as a function of the local Reynolds number.

## 6. REFERENCES

- Girardi, R.M. & Bizarro, A.F., 1995, Modification of the Hess& Smith Method for calculating cascades and airfoils with cusped trailing edge, XIII Congresso Brasileiro de Engenharia Mecânica, 12 a 15 de Dezembro, Belo Horizonte, MG, Brasil.
- Hess, J.L. & Smith, A.M.O., 1966, Calculation of potential flow about arbitrary bodies. Progress in Aeronautical Sciences, Vol. 8, Pergamon Press, 1966.
- Jacob, H., G., 1982, Rechnergestuetzte Optimierung sticher and dynamischer Systeme – Beispiele mit FORTRAN-Programmen, Springer-Verlag, Berlin, B. R. Deutschland.
- Karamcheti, K., 1980, Principles of ideal-fluid aerodynamics, Robert Krieger Publ. Co., Malabar, Fla.
- Roskam, J., 1985, Airplane Design: parts I-VIII, Roskam Aviation and Engineering Corporatio, Ottawa, Kansas.
- Schlichting, H. & Truckenbrodt, E., 1979, Aerodynamics of the airplane, McGraw-Hill, New York.